IOPscience iopscience.iop.org

Home Search Collections Journals About Contact us My IOPscience

Superposed second-harmonic Talbot self-image from a PPLT crystal

This content has been downloaded from IOPscience. Please scroll down to see the full text.

2014 Laser Phys. Lett. 11 095402

(http://iopscience.iop.org/1612-202X/11/9/095402)

View the table of contents for this issue, or go to the journal homepage for more

Download details:

IP Address: 210.28.139.26
This content was downloaded on 08/06/2015 at 07:47

Please note that terms and conditions apply.

IOP Publishing | Astro Ltd Laser Physics Letters
Laser Phys. Lett. **11** (2014) 095402 (5pp) doi:10.1088/1612-2011/11/9/095402

Superposed second-harmonic Talbot self-image from a PPLT crystal

Dunzhao Wei[1], Dongmei Liu[1], Xiaopeng Hu[1], Yong Zhang[1] and Min Xiao[1,2]

[1] National Laboratory of Solid State Microstructures, College of Engineering and Applied Sciences, School of Physics, Nanjing University, Nanjing 210093, People's Republic of China
[2] Department of Physics, University of Arkansas, Fayetteville, AR 72701, USA

E-mail: zhangyong@nju.edu.cn and mxiao@uark.edu

Received 10 April 2014, revised 5 June 2014
Accepted for publication 15 June 2014
Published 4 July 2014

Abstract
We experimentally demonstrate the superposed second-harmonic Talbot self-image in a z-cut periodically-poled $LiTaO_3$ crystal. The generated second-harmonic (SH) waves in the positive and negative domains have the same intensity but different phases (a phase shift of π) due to the opposite poling directions, i.e. a second-harmonic phase pattern is generated from the crystal. By introducing a reference SH wave, we can selectively study the self-imaging originating from the SH patterns with different phases. In the integer and fractional Talbot planes, the two patterns interfere with each other and form superposed self-imaging patterns.

Keywords: Talbot self-imaging, second-harmonic, PPLT crystals

(Some figures may appear in colour only in the online journal)

1. Introduction

The conventional Talbot effect, also called self-imaging or lensless imaging, was first discovered by Henry Fox Talbot [1] in 1836 and proved by Lord Rayleigh [2] in 1881. It is a special case of the Fresnel imaging phenomenon referring to the self-imaging of a grating or other periodic structures at a certain imaging distance (i.e. the Talbot distance) without any other optical imaging components. Owing to its unique characteristics, the Talbot effect has been extensively applied in optical testing, optical metrology [3, 4], array illuminator [5–8], photo-lithography [9, 10], holographic multiplexing storage [11] and so on [12, 13]. What's more, the optical Talbot effect has also been extended to other areas recently, such as the multicolor Talbot effect in waveguide arrays [14, 15], mid-infrared array illuminator [16], the quantum Talbot effect [17], electron Talbot interferometer [18], and x-ray phase imaging [19].

The nonlinear Talbot effect [20] was first reported in a *z*-cut periodically-poled $LiTaO_3$ (PPLT) crystal which has been widely used to enhance the nonlinear optical processes [21–24]. The second-harmonic (SH) intensity generated at the domain walls is different from that inside the domains because the nonlinear coefficients near the domain walls are changed due to the crystal's distortion. Therefore, a periodic SH pattern presents at the end face of the crystal, and fulfills the necessary condition to realize self-imaging. Because the nonlinear Talbot effect relates to the second-order nonlinear tensor, it has several unique characteristics compared to the Talbot effect in linear optics. For example, no real grating is required and the resolution is improved due to frequency-doubling. The theory of the conventional Talbot effect [2] has to be modified to explain this nonlinear Talbot effect [25, 26]. Moreover, the nonlinear Talbot effect can be modulated by the quasi-phase-matching (QPM) method [27] or by applying an external field to the crystal [28].

Up to now, study of the nonlinear Talbot effect has focused on the intensity patterns of the SH waves. However, the phase of the generated SH self-imaging—which needs to be studied to better understand its features, which originate from the nonlinear optical process—has not been explored. In PPLT crystals, the positive and negative domains have antiparallel ferroelectric polarizations, which results in a π phase shift in the generated SH waves coming from these two domain areas [29]. Then, the SH waves with different phases interfere with each other and compose various periodic intensity patterns at different imaging planes, as previously reported [20]. In this letter, we demonstrate how the SH patterns with different phases evolve, self-image, and superpose with each other, by introducing a reference SH beam.

 © 2014 Astro Ltd Printed in the UK

2. Theory

The sample in our experiment is a z-cut two-dimensional (2D) squarely-poled PPLT crystal with a period of $d = 5.5\,\mu$m and a duty cycle of ~ 54.5% as shown in figure 1(a). The sample was fabricated by applying an electric field on a single-domain $LiTaO_3$ (LT) crystal. As shown in figure 1(b), the crystal's physical axes (x_1, x_2, x_3) of a positive domain are set to coincide with the lab axes (x, y, z). When the domain is inverted to negative—the equivalent of a rotation of 180° around the x lab axis [29]—the crystal's axes become parallel to (x, $-y$, $-z$). The ferroelectric polarization $\mathbf{P}_s$ is parallel to the z (or $-z$) axis in positive (or negative) domains. Obviously, such a poling process means that the optical second-order nonlinear tensor of the nonlinear crystal was operated on by a transformation matrix a_{ij} defined by [29]

$$a_{ij} = \begin{bmatrix} 1 & 0 & 0 \\ 0 & -1 & 0 \\ 0 & 0 & -1 \end{bmatrix}. \tag{1}$$

It is easy to show that all the nonlinear coefficients have different signs in different domains.

First, consider a positive domain. The fundamental light polarizes in the x–y plane and propagates along the z direction [30]. The direction of its electric field is indicated by an angel φ with respect to the x lab axis (figure 1(b)). So it has (x_1, x_2, x_3) components, also (x, y, z) components with $\boldsymbol{E} = (E_0 \cos\varphi, E_0 \sin\varphi, 0)$, which can induce a nonlinear polarization of:

$$\boldsymbol{P}(2\omega) = \left(-d_{22}E_0^2 \sin 2\varphi \quad -d_{22}E_0^2 \cos 2\varphi \quad -d_{31}E_0^2\right). \tag{2}$$

So the intensity of the SH wave travelling along the z-axis is given by:

$$\begin{cases} \mathrm{I}_x(2\omega) \propto \left(d_{22}E_0^2 \sin 2\varphi\right)^2 \\ \mathrm{I}_y(2\omega) \propto \left(d_{22}E_0^2 \cos 2\varphi\right)^2 \end{cases}. \tag{3}$$

Its polarization is along the orientation defined by ($3\pi/2 - 2\varphi$) relative to the x-axis (figure 1(c)). Analogously, in a negative domain, the electric field has (x_1, x_2, x_3) components with $\boldsymbol{E} = (E_0 \cos\varphi, -E_0 \sin\varphi, 0)$, inducing a nonlinear polarization of:

$$\boldsymbol{P}(2\omega) = \left(d_{22}E_0^2 \sin 2\varphi \quad -d_{22}E_0^2 \cos 2\varphi \quad -d_{31}E_0^2\right). \tag{4}$$

In the lab axes (x, y, z), equation (4) turns into:

$$\boldsymbol{P}(2\omega) = \left(d_{22}E_0^2 \sin 2\varphi \quad d_{22}E_0^2 \cos 2\varphi \quad -d_{31}E_0^2\right). \tag{5}$$

The intensity of the SH wave can also be written as in equation (3), and its polarization is ($\pi/2 - 2\varphi$) relative to the x-axis (figure 1(c)). It is easy to show that the intensities of the SH waves are the same in both positive and negative domains. However, the initial phases of the SH waves from the positive and negative domains have a relative shift of π. Obviously, it is difficult to distinguish the phases in the SH patterns solely based on the intensity image. However, if we introduce a reference SH wave, which has a uniform spatial phase distribution, to interfere with the SH pattern from the PPLT crystal, it will be easy to measure the phase differences. This method has been previously used to map the domains in ferroic materials [31, 32].

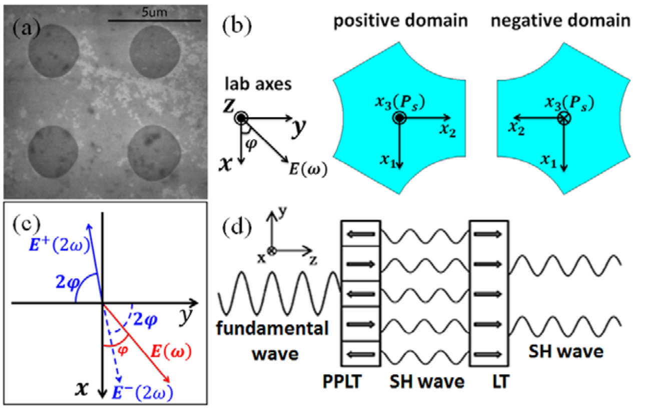

Figure 1. (a) SEM photo of the PPLT crystal. The circular areas correspond to the positive domains and the background is the negative domain. (b) Schematic diagrams of a positive domain and a negative domain in the x–y plane. (x_1, x_2, x_3) are the crystal's physical axes, (x, y, z) are the lab axes; $\mathbf{P}_s$ is the polarization direction of the ferroelectric domain, and $\boldsymbol{E}(\omega)$ is the electric field of the input light. (c) The polarization directions of the generated second-harmonic waves in positive ($\boldsymbol{E}^+(2\omega)$) and negative ($\boldsymbol{E}^-(2\omega)$) domains. ($d$) Scheme of the experimental setup. The fundamental beam produces a SH phase pattern in the PPLT crystal, which interferes with the reference SH beam coming from the LT crystal.

In our experiment, we used a z-cut plain (unpoled) LT crystal to generate a reference SH signal, which was placed in close proximity to the PPLT crystal. The thickness of the LT crystal is equal to that of the PPLT crystal, so that the reference SH intensity is almost the same as that generated in the PPLT crystal. Here, the consumption of the fundamental power can be neglected because of the low conversion efficiency. When the crystal's axes of the LT crystal coincide with the lab axes in figure 1(b), the reference SH signal has the same phase as that in the positive domain of the PPLT crystal. Then, the SH wave from the positive domain can be enhanced, by constructive interference, while the SH wave from the negative domain almost vanishes due to destructive interference.

The phase of the reference SH wave can be changed by flipping the LT crystal. However, this is not convenient in our experimental setup. We used an alternative method to change the phase of the reference wave. It can be deduced from equations (2) and (5) that, through changing the sign of d_{22}, the phase of the SH wave travelling along the z-axis can also be shifted by a value of π. Because the LT crystal has a 3 m point group, we can change the sign of d_{22} by rotating the crystal around the lab z-axis by an angle of 60°. This rotation operation corresponds to the case that the nonlinear tensor is operated on by a transformation matrix a_{ij}:

$$a_{ij} = \begin{bmatrix} -1 & 0 & 0 \\ 0 & -1 & 0 \\ 0 & 0 & 1 \end{bmatrix}. \tag{6}$$

After a 60° rotation, the nonlinear coefficient d_{22} turns into $-d_{22}$ in the same lab axes. This causes a π phase shift in the reference SH wave, which then interferes constructively with the SH wave from the negative domain. Hence, the

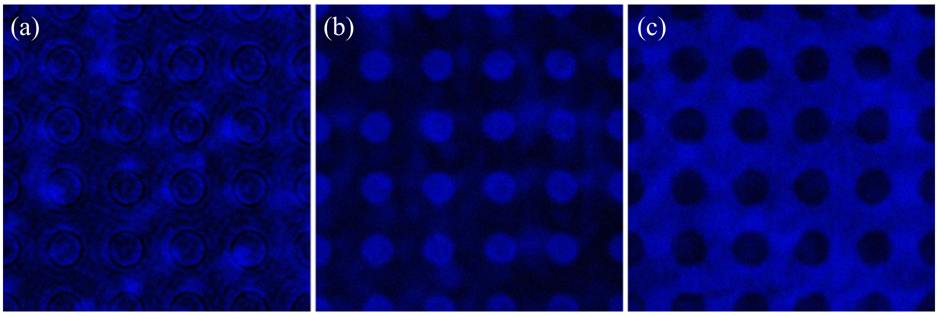

Figure 2. The SH patterns at the end face of the PPLT crystal. (*a*) No reference SH beam is introduced. (*b*) and (*c*) correspond to the situations that the reference SH beam constructively interfere with the SH patterns from positive and negative domains, respectively.

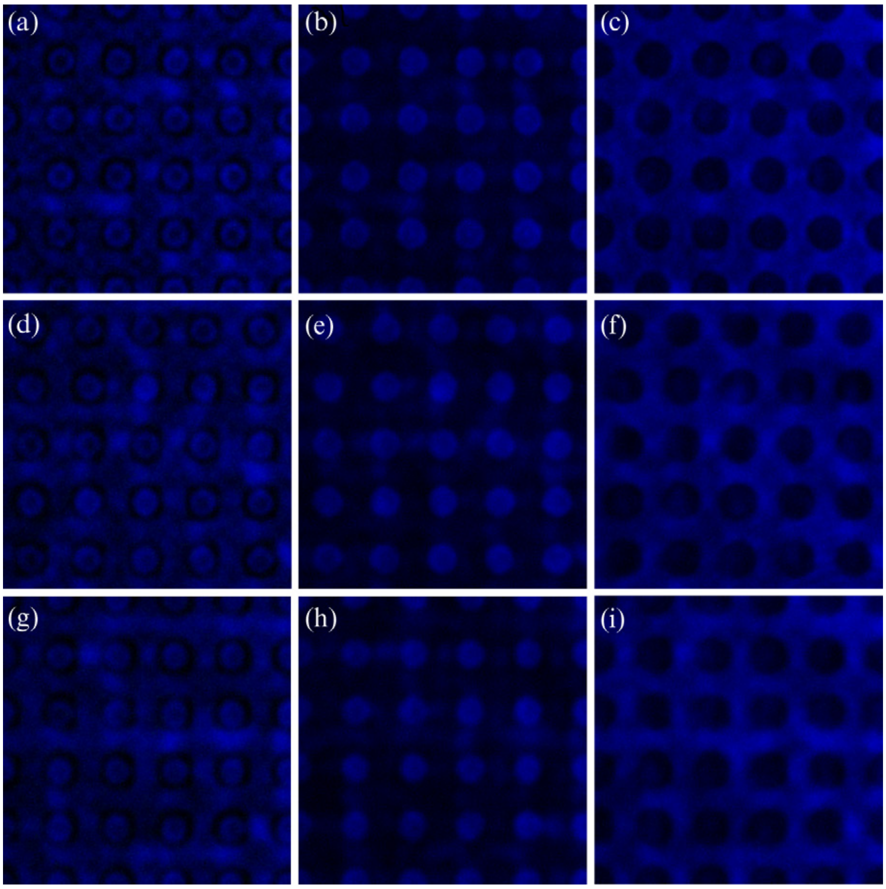

Figure 3. The superposed SH Talbot self-imaging patterns. (*a*), (*d*) and (*g*) show the Talbot effect without introducing a reference beam. (*b*), (*e*) and (*h*) are self-images of the SH pattern, generated from the positive domains. (*c*), (*f*) and (*i*) are self-imaging patterns of the SH waves from the negative domains. From the top down, the three rows correspond to the first Talbot plane, the 3/2 Talbot plane and the second Talbot plane, respectively.

SH patterns with different phases (i.e. produced in different domains) from the PPLT crystal can be selectively studied.

3. Experimental results

As shown in figure 1(*d*), the fundamental light from a Ti:Sapphire femtosecond laser with a wavelength of $\lambda = 900$ nm was focused on the sample along the lab *z*-axis. Its polarization is along the lab *x*-axis. The PPLT crystal was placed so that the physical axes of the positive domain coincide with the lab axes (figure 1(*b*)). The ferroelectric polarization of the LT crystal was parallel to the propagation direction of the fundamental beam. After filtering out the fundamental wave with a short-pass optical filter, the SH signals were magnified by an objective (100X, N.A. = 0.7) and recorded on a CCD camera.

Figure 2 shows the SH intensity patterns at the end face of the PPLT crystal. First, we removed the LT crystal and collected all the forward SH waves. The recorded SH intensity pattern is shown in figure 2(*a*). The periodic dark rings correspond to the domain walls. The weak SH signals near the domain walls can be attributed to the distorted crystal lattice. One can also find that the background is not uniform in figure 2(*a*), which could result from the non-perfect domain

Table 1. The calculated and measured positions of different Talbot planes.

Talbot plane $4d^2/\lambda \times (mn^{-1})$	Calculated measured values (μm)	Measured values (μm)
1	134.4	133.5
3/2	201.7	198.8
2	268.9	265.0

structure. Such a periodic SH pattern can be used to realize Talbot self-imaging, as reported in [20]. Figures 3(*a*), (*d*) and (*g*) are the SH images at the first Talbot plane, the 3/2 Talbot plane, and the second Talbot plane, respectively, which were recorded by moving the objective. The Talbot length of a square array can be deduced from $Z_t = 4d^2/\lambda$, where λ is the wavelength of the fundament light and d the structure period. The measured and calculated positions of different Talbot planes are well consistent with each other as shown in table 1. For instance, the calculated Talbot length is 134.4 μm while the measured value is 133.5 μm.

Next, we put the LT crystal in a position next to the PPLT crystal. At first, the position of the objective was carefully adjusted to image the end face of the PPLT crystal. When the fundamental beam travels through the LT crystal, a reference SH wave with a uniform spatial phase distribution is generated, which interferes with the SH wave produced in the PPLT crystal. Because the refractive indices in PPLT and LT crystals are the same, and the reference SH wave is generated by the same fundamental beam, the interference between the SH beam from the PPLT crystal and the reference SH beam results in a clear and stable pattern. Figure 2(*b*) presents the interference pattern when the physical axes of the LT crystal coincide with the lab axes. In this case, the reference SH wave has the same phase as that in the positive domain of the PPLT crystal. Because of constructive interference, an array consisting of lots of SH spots, which originate from the positive domains in the PPLT crystal, is observed (figure 2(*b*)). The background is dark due to the destructive interference between the reference SH beam and the SH wave from the negative domains in the PPLT crystal. Figure 2(*b*) provides clear evidence that the SH pattern from the PPLT crystal (figure 2(*a*)) consists of two different phases. The periodic SH spots in figure 2(*b*), which share the same phase, also fulfill the necessary condition of self-imaging. Figures 3(*b*), (*e*) and (*h*) shows the Talbot images at 1, 3/2, and 2 Talbot lengths, respectively. The unique characteristics of the self-imaging effect, such as a half-period lateral shift at the 3/2 Talbot plane, are also observed by carefully comparing figures 3(*b*) and (*e*).

When we rotate the LT crystal around the z-axis by an angle of 60°, a π phase shift is introduced into the reference SH wave, as discussed in section 2. As a result, constructive interference occurs between the reference SH beam and the SH pattern from the negative domains in the PPLT crystal. Now the SH pattern from the negative domains can be distinguished, as shown in figure 2(*c*). A lot of dark holes appear at a bright SH background because of the destructive interference between the reference SH wave and the SH wave from the circular positive domains. Such a SH pattern can also realize self-imaging. For instance, self-imaging happens at the first and second Talbot lengths, as shown in figures 3(*c*) and (*i*), respectively. Figure 3(*f*) at the 3/2 Talbot plane also exhibits a lateral shift, as predicted.

We have, therefore, demonstrated that the SH image from the PPLT crystal actually includes two sets of SH patterns with different phases, which can separately realize Talbot self-imaging. It is obvious that the superposition between them can result in the nonlinear Talbot effect reported in [20]. However, it is not a simple summation of their intensities. The different phases from positive and negative domains also has an important impact on the superposition. For example, figure 3(*a*) is a superposed self-image of figures 3(*b*) and (*c*). In figure 3(*a*), one can find a small dark point inside each SH spot from the positive domains. However, such a dark point is not clear in figure 3(*b*). The answer may lie in the dark holes in figure 3(*c*). After careful observation, one finds that the dark hole is not totally dark. There are weak SH waves inside the dark holes in figure 3(*c*), which could destructively interfere with the bright spots in figure 3(*b*) when superposed and generate the dark points seen in figure 3(*a*). Similar phenomena can also be found in other Talbot planes.

The technique reported here provides a potential method for separately inspecting the qualities of the positive and negative domain in PPLT crystals, which makes it easier to locate defects and imperfections in the structure. Another possible application is to make a compact Talbot illuminator which can generate two sets of arrays. The superposed Talbot effect can be used to generate a cleaner periodic SH array (see figures 3(*b*), (*e*) and (*h*)), which can work as a coupler for an optical fiber array [33].

4. Conclusion

We have investigated the superposed SH Talbot self-imaging patterns involving phase information from a PPLT crystal. By introducing a reference SH wave, two sets of periodic phase patterns are decomposed from the SH pattern at the end face of the PPLT crystal, which can evolve along the propagation direction and realize self-imaging at the Talbot planes, separately. Their superposition can result in the previously reported nonlinear Talbot effect [20]. Our experimental results provide a better understanding of the nonlinear Talbot effect from PPLT crystals, which not only enables self-imaging of the intensity patterns, but also revives the periodic phase distributions. Such superposed Talbot self-imaging has potential applications in domain inspection, lithography, illuminators, fiber couplers, and so on.

Acknowledgment

This work was supported by the National Basic Research Program of China (Nos. 2012CB921804 and 2011CBA00205), the National Science Foundation of China (Nos. 11274162, 61222503, 11274165, 11321063), and the New Century

Excellent Talents in University. The authors thank Jianming Wen for useful discussions.

References

[1] Talbot H F 1836 *Phil. Mag.* **9** 401–7
[2] Rayleigh L 1881 *Phil. Mag.* **11** 196–205
[3] Lohmann A W and Silva D E 1971 *Opt. Commun.* **2** 413–5
[4] Kothiyal M P and Sirohi R S 1987 *Appl. Opt.* **26** 4056–57
[5] Lohmann A W and Thomas J A 1990 *Appl. Opt.* **29** 4337–40
[6] Xi P, Zhou C H, Dai E W and Liu L R 2002 *Opt. Lett.* **27** 228–30
[7] Paturzo M, Natale P D, Nicola S D, Ferraro P, Mailis S, Eason R W, Coppola G, Iodice M and Gioffre M 2006 *Opt. Lett.* **31** 3164–66
[8] Zhang J H and Chen Y L 2013 *IEEE J. Quantum Electron.* **49** 471–6
[9] Lsoyan A, Jiang F, Cheng Y C, Cerrina F, Wachulak P, Urbanski L, Rocca J, Menoni C and Marconi M 2009 *J. Vac. Sci. Technol.* B **27** 2931–7
[10] Stuerzebecher L, Harzendorf T, Vogler U, Zeitner U D and Voelkel R 2010 *Opt. Express* **18** 19485–94
[11] Zhou C H, Stankovic S, Denz C and Tschudi T 1999 *Opt. Commun.* **161** 209–11
[12] Patorski K 1989 *Prog. Opt.* **27** 1–108
[13] Wen J M, Zhang Y and Xiao M 2013 *Adv. Opt. Photon.* **5** 83–130
[14] Garanovich I L, Sukhorukov A A and Kivshar Y S 2006 *Phys. Rev.* E **74** 066609
[15] Garanovich I L 2008 *Phys. Lett.* A **372** 3922–25
[16] Maddaloni P, Paturzo M, Ferraro P, Malara P, Natale P D, Gioffre M, Coppola G and Iodice M 2009 *Appl. Phys. Lett.* **94** 121105
[17] Song X B, Wang H B, Xiong J, Wang K, Zhang X, Luo K H and Wu L A 2011 *Phys. Rev. Lett.* **107** 033902
[18] McMorran B J and Cronin A D 2009 *New J. Phys.* **11** 033021
[19] Weitkamp T, Diaz A, David C, Pfeiffer F, Stampanoni M, Cloetens P and Ziegler E 2005 *Opt. Exp.* **13** 6296–304
[20] Zhang Y, Wen J M, Zhu S N and Xiao M 2010 *Phys. Rev. Lett.* **104** 183901
[21] Fejer M M, Magel G A, Jundt D H and Byer R L 1992 *IEEE J. Quantum Electron.* **28** 2631–54
[22] Myers L E, Eckardt R C, Fejer M M and Byer R L, Bosenberg W R and Pierce J W 1995 *J. Opt. Soc. Am.* B **12** 2102–16
[23] Broderick N G R, Ross G W, Offerhaus H L, Richardson D J and Hanna D C 2000 *Phys. Rev. Lett.* **84** 4345–48
[24] Shapira A and Arie A 2011 *Opt. Lett.* **36** 1933–35
[25] Wen J M, Zhang Y, Zhu S N and Xiao M 2011 *J. Opt. Soc. Am.* B **28** 275–80
[26] Chen Z H, Liu D M, Zhang Y, Wen J M, Zhu S N and Xiao M 2012 *Opt. Lett.* **37** 689–91
[27] Liu D M, Wei D Z, Zhang Y, Zhou J, Hu X P, Zhu S N and Xiao M 2013 *Opt. Express* **21** 013969
[28] Liu DM, Zhang Y, Chen Z H, Wen J M and Xiao M 2012 *J. Opt. Soc. Am.* B **29** 3325–29
[29] Lu Y Q, Wan Z L, Wang Q, Xi Y X and Ming N B 2000 *Appl. Phys. Lett.* **77** 3719
[30] Denev S A, Lummen T A, Barnes E, Kumar A and Gopalan V 2011 *J. Am. Ceram. Soc.* **94** 2699–727
[31] Fiebig M, Lottermoser T, Fröhlich D, Goltsev A V and Pisarev R V 2002 *Nature* **419** 818–20
[32] Van Aken B B, Rivera J P, Schmid H and Fiebig M 2007 *Nature* **449** 702–5
[33] Mortimore D B and Arkwright J W 1991 *Appl. Opt.* **30** 650–9